Analyzing Social Distancing and Seasonality of COVID-19 with Mean Field Evolutionary Dynamics

Hao Gao*, Wuchen Li†, Miao Pan*, Zhu Han* and H. Vincent Poor‡
*Department of Electrical and Computer Engineering, University of Houston, Houston, TX, USA
†Department of Mathematics, University of South Carolina, Columbia, SC, USA
‡Department of Electrical Engineering, Princeton University, Princeton, NJ, USA

2020 IEEE Globecom Workshops (GC Wkshps) | 978-1-7281-7307-8/20/$31.00 ©2020 IEEE | DOI: 10.1109/GCWkshps50303.2020.9367567

***Abstract*—The outbreak of the coronavirus pandemic since the end of 2019 has been declared as a world health emergency by the World Health Organization, which raised the importance of an accurate mathematical epidemiological dynamic model to predict the evolution of COVID-19. Replicator dynamics (RDs) are exclusively applied to many epidemic models, but they fail to satisfy the Nash stationarity and can only describe a unidirectional population flow between different states. In this paper, we proposed mean field evolutionary dynamics (MFEDs), inspired by the optimal transport theory and mean field games on graphs, to model epidemic dynamics. We compare the MFEDs with RDs theoretically. In particular, we also show the efficiency of MFEDs by modeling the evolution of COVID-19 in Wuhan, China. Furthermore, we analyze the effect of one-time social distancing as well as the seasonality of COVID-19 through the post-pandemic period.**

I. Introduction

The third zoonotic human coronavirus of the century, which is named the SARS-CoV-2, emerged at the end of 2019, having a wide-ranging and severe impact upon many aspects of our society, especially health, finance, and social life [1]. For example, from February 24th to February 28th, stock markets worldwide reported their largest one-week declines since the 2008 financial crisis, thus entering a correction. Moreover, the disease COVID-19 has posed great threat on human lives worldwide. As of 10th August 2020, 19,869,127 infected cases and 731,453 deaths have been confirmed due to the COVID-19 pandemic [2] [3]. In order to mitigate the impact on financial markets and human lives, prediction of the evolution of COVID-19 within the human population with an accurate mathematical epidemic dynamical models is of vital importance.

A. Related Work

Epidemic Models: The Kermack–McKendrick model [4] is one of the classic epidemic models, which divides the population into three main categories: susceptible, infected, and recovered (SIR) individuals. The strategy graph of the SIR model is shown in Fig. 1a. The classic SIR epidemic model has been extended into many distinct epidemic models by adding new individual states. The authors of [5] have extended the classic SIR model into the SIVR epidemic model as shown in Fig. 1b, where "V" denotes the "variation" state. The "variation" state can characterize the mutation behaviors of influenza viruses during their spreading process. The authors of [6] considered the continuous-time epidemic model with sub-populations of susceptible-exposed-infected-recovered (SEIR) under a general feedback vaccination control rule. The authors of [7] further extended the SEIR model into the discrete SEIADR (acronym: susceptible (S), exposed (E), symptomatic infectious (I), asymptomatic infectious (A), dead infectious (D) and recovered (R)) epidemic model, by incorporating the asymptomatic infectious and the lying infective bodies as infectious extra populations on the standard populations of SEIR type models. Several controls are given under the SEIADR model, such as vaccination treatment and the removal of infective lying corpses. In this paper, we model the transmission of COVID-19 in the SIDR model, extended from the SIR model by adding the "D" state to represent the dead cases.

Epidemic Dynamics. To our best knowledge, the replicator dynamics (RD), introduced in the mathematical biology literature by Taylor and Jonker [8], are exclusively utilized to describe the epidemic evolution under distinct epidemic models. Based on imitation, RDs require very limited information: each agent only needs to know its payoff to the current state/strategy. However, RDs fail the Nash stationarity, as they admit boundary rest points that are not a Nash equilibrium.

There are other evolutionary dynamics, which have the potential to describe the epidemic evolution, even though they have not been used in any epidemic models yet. The best response dynamics [9] satisfy the Nash stationarity, i.e., the rest points always coincide with the Nash equilibrium. However, the protocol that generates these dynamics are discontinuous, requiring information of the payoffs to all available strategies to obtain the current best response. The Brown-von Neumann-Nash (BNN) dynamics [10] satisfy the Nash stationarity, and are established on continuous revision protocols. But these protocols also requires that agents know the average payoff, which should be provided by a central source. Finally, the pairwise comparison dynamics, first appeared in the transportation science literature by M. J. Smith [11], latter developed by Sandholm [12], satisfy Nash stationarity while only make the limited informational demand: payoffs to the

This work is partially supported by US Multidisciplinary University Research Initiative 18RT0073, NSF EARS-1839818, CNS1717454, CNS-1731424, and CNS-1702850

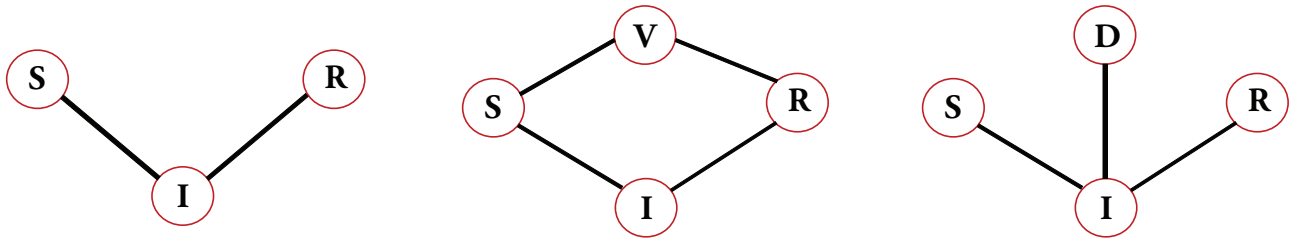

(a) SIR Epidemic Model (b) SIVR Epidemic Model (c) SIDR Epidemic model

Fig. 1: Strategy graphs for distinct epidemic models

current strategies and randomly chosen candidate strategies. The novel epidemic dynamics that we propose in this paper falls into the category of pairwise comparison dynamics.

B. Motivations and Contributions

The RDs have the following drawbacks when used to model the transmission of COVID-19: (i) the RDs fail to satisfy the Nash stationarity, which means that the final equilibrium is not guaranteed to be a stable state of the epidemic, (ii) the population flow between different states is unidirectional, which is contradicted to the realistic situation [13]. Since in real life, infected individuals are not guaranteed to get immunity, and thus become susceptible again. This common behavior of epidemic requires that the dynamics should allow bidirectional population flow between states. Therefore, we propose the mean field evolutionary dynamics (MFED) as a novel epidemic dynamics.

The main contributions of this paper are summarized as follows:

- We propose the MFED as a novel epidemic dynamics and compare it with the RD theoretically.
- We design the SIDR model and achieve a good fitting into the statistics of COVID-19 in Wuhan, China.
- We analyze the effect of one-time social distancing and the seasonality of COVID-19 through the post-pandemic period.

The remainder of this paper is organized as follows. In Section II, we propose RDs in the SIDR epidemic model, and derive the corresponding payoff functions. In Section III, we propose the MFEDs in the SIDR model and compare it with RDs theoretically. In Section IV, we model the evolution of COVID-19 in Wuhan, China with MFEDs. Section V concludes the paper.

II. Replicator Dynamics

A. Preliminaries of Population game on Graph

In order to give the general form of RDs, we need to clarify the following fundamental concepts. We consider a population game on graph $\mathcal{G} = (\mathcal{S}, \mathcal{E})$:

- **Nodes and Edges:** Nodes of this graph are pure strategies from the discrete strategy set $\mathcal{S} = \{1, 2, \cdots, s\}$. Edges are connections between nodes. Node $i \in \mathcal{S}$ and node $j \in \mathcal{S}$ are able to form an edge $(i, j) \in \mathcal{E}$ if players can directly switch from strategy i to strategy j.
- **Neighborhood:** The neighborhood of node i is the set of all nodes which have a direct connection to node i. It is defined as follows:

$$N(i) = \{j \in \mathcal{S} : (i, j) \in \mathcal{E}\}.$$

- **Population State Space:** The population state space consists of all available population distribution on the discrete strategy set $\mathcal{S}$ and it is defined in the following way:

$$\mathcal{P}(\mathcal{S}) = \{(\rho_i)_{i=1}^s : \sum_{i=1}^s \rho_i = 1, \rho_i \geq 0, i \in \mathcal{S}\}, \quad (1)$$

where ρ_i represents the fraction of population selecting strategy i. The interior of $\mathcal{P}(\mathcal{S})$ is denoted as $\mathcal{P}_o(\mathcal{S})$.
- **Payoff Function:** The payoff function to strategy i, $F_i : \mathcal{P}(\mathcal{S}) \to \mathbb{R}$ is a mapping from the current population distribution to the reward of selecting strategy i. Each agent is only interested in maximizing its own reward by selecting different strategies.

B. Replicator Dynamics in General Form

The RD, introduced in the mathematical biology literature by Taylor and Jonker [8], are the most thoroughly studied evolutionary dynamics and have been widely regarded as the epidemic dynamics in many epidemic models. Their general expression is given by

$$\frac{d\rho_i}{dt} = \rho_i(F_i(\rho) - \bar{F}(\rho)), \quad (2)$$

where ρ_i represents the fraction of population selecting strategy i, $\rho = (\rho)_{i=1}^s$ is the population distribution on all strategies, $F_i : \mathcal{P}(\mathcal{S}) \to \mathbb{R}$ is the payoff to strategy i, and $\bar{F}(\rho) = \sum_{i=1}^s \rho_i F_i(\rho)$ is the average payoff of the whole population. Under these dynamics, the growth rate of the population on each strategy i is equivalent to its excessive payoff, i.e., to the difference between its payoff and the average payoff of the population. Intuitively, if the payoff of a given strategy is higher than the average, it will be selected by more agents as every individual in the population is trying to maximize his/her own payoff.

C. Replicator Dynamics in the SIDR Model

Denoting the number of susceptible population as ρ_s, the number of infected population as ρ_I, the number of recovered population as ρ_r, and the number of dead population as ρ_d, the RDs, which describe the evolution of the epidemic in the SIDR model, are

$$\begin{aligned} \frac{d\rho_s}{dt} &= -\eta\rho_s\rho_I, \\ \frac{d\rho_I}{dt} &= \eta\rho_s\rho_I - \epsilon_1\rho_I - \epsilon_2\rho_I, \\ \frac{d\rho_r}{dt} &= \epsilon_1\rho_I, \\ \frac{d\rho_d}{dt} &= \epsilon_2\rho_I, \end{aligned} \tag{3}$$

where η, ϵ_1, ϵ_2 are the infection rate, recovery rate, and death rate of COVID-19, respectively. It is developed based on the following assumptions: (i) The total population size is the constant N. (ii) One infected individual can make enough contact with ηN others to transmit infection per unit time, where η is the infection rate. (iii) Infected individuals recover from the disease and get permanent immunity at rate $\epsilon_1\rho_I$ per unit time. (iv) Infected individuals die at rate $\epsilon_2\rho_I$ per unit time. The strategy graph for the SIDR model is shown in Fig. 1c.

D. Payoff Functions in the SIDR Model

We now derive the payoff functions to each state/strategy in the SIDR model. Comparing (3) with the general form in (2), we obtain the following equations:

$$\begin{aligned} -\eta\rho_s\rho_I &= \rho_s(F_s(\rho) - \bar{F}(\rho)), \\ \eta\rho_s\rho_I - \epsilon_1\rho_I - \epsilon_2\rho_I &= \rho_I(F_I(\rho) - \bar{F}(\rho)), \\ \epsilon_1\rho_I &= \rho_r(F_r(\rho) - \bar{F}(\rho)), \\ \epsilon_2\rho_I &= \rho_d(F_d(\rho) - \bar{F}(\rho)), \end{aligned} \tag{4}$$

where F_s, F_I, F_r, and F_d are the payoffs when an individual becomes susceptible, infected, recovered, and dead, respectively. $\rho = [\rho_s, \rho_I, \rho_r, \rho_d]$ is a vector recording the number of all sub-populations. $\bar{F}(\rho)$ is the average payoff of the whole population. Solving equation systems in (4), we obtain the payoff functions for the SIDR model as follows:

$$\begin{aligned} &F_s = -\eta\rho_I, \ F_I = \eta\rho_s - \epsilon_1 - \epsilon_2, \\ &F_r = \frac{\epsilon_1\rho_I}{\rho_r}, \ F_d = \frac{\epsilon_2\rho_I}{\rho_d}. \end{aligned} \tag{5}$$

III. Mean Field Evolutionary Dynamics

A. Mean Field Evolutionary Dynamics in the SIDR Model

The MFED, thoroughly analyzed in [14], [15], is an evolutionary dynamics for population games with discrete strategy sets. It is originally inspired by the optimal transport theory [16], [17] and mean field game [18], [19], [20]. The general form of MFED is given in theorem 1.

Theorem 1. *Suppose that a population game has strategy graph $\mathcal{G} = (\mathcal{S}, \mathcal{E})$ and the constant $\beta \geq 0$, the payoff function $F_i : \mathcal{P}(\mathcal{S}) \to \mathbb{R}$ are continuous. Then for any initial condition $\rho^0 \in \mathcal{P}_o(\mathcal{S})$, the Fokker-Planck equation*

$$\begin{aligned} \frac{\mathrm{d}\rho_i}{\mathrm{d}t} = &\sum_{j\in N(i)} \omega_{ij}\rho_j[F_i(\rho) - F_j(\rho) + \beta(\log\rho_j - \log\rho_i)]^+ \\ &- \sum_{j\in N(i)} \omega_{ij}\rho_i[F_j(\rho) - F_i(\rho) + \beta(\log\rho_i - \log\rho_j)]^+ \end{aligned} \tag{6}$$

are evolutionary dynamics in $\mathcal{P}_o(\mathcal{S})$. $\beta \geq 0$ represents the strength of uncertainty, $[\cdot]^+ = max\{\cdot, 0\}$, $N(i)$ is the neighborhood of node i and ω_{ij} is the weight on edge (i, j).

Detailed proof of Theorem 1 has been provided in [14]. The MFED, proposed in Theorem 1, are pairwise comparison evolutionary dynamics [12]. Unlike the RD, MFED sets the probability of switching from the current strategy i to strategy j proportional to the differences between these strategies' payoffs. One agent will compare its current payoff with the payoffs of the strategies in its neighborhood to determine whether it will switch.

With Theorem 1 and payoff functions in (5), we can derive the MFEDs in the SIDR model. Following the strategy graph in Fig. 1c and substituting the payoffs functions (5) into (6) ($\omega_{ij} = 1, \beta = 0$), we obtain the MFEDs for the SIDR model as follows:

$$\begin{aligned} \frac{d\rho_s}{dt} =& \rho_I[F_s - F_I]^+ - \rho_s[F_I - F_s]^+, \\ \frac{d\rho_I}{dt} =& \rho_s[F_I - F_s]^+ + \rho_r[F_I - F_r]^+ + \\ & \rho_d[F_I - F_d]^+ - \rho_I[F_s - F_I]^+ - \\ & \rho_I[F_r - F_I]^+ - \rho_I[F_d - F_I]^+, \\ \frac{d\rho_r}{dt} =& \rho_I[F_r - F_I]^+ - \rho_r[F_I - F_r]^+, \\ \frac{d\rho_d}{dt} =& \rho_I[F_d - F_I]^+ - \rho_d[F_I - F_d]^+. \end{aligned} \tag{7}$$

With the MFEDs in (7), we allow a bidirectional population flow between distinct states, i.e., we can remove the unrealistic assumptions, required by RDs, that the infected individuals can always get permanent immunity after recovery.

B. Comparison with Replicator Dynamics

Both the RD and the MFED will lead the population game to a Nash equilibrium, where there is no incentive for agents to change their strategies unilaterally. From the perspective of epidemic evolution, the Nash equilibrium will be a stable state of a generic epidemic. The definition of a Nash equilibrium is as follows.

Definition 1. *State ρ_n is a Nash equilibrium of a population game P ($\rho_n \in NE(P)$) if each strategy in use at ρ_n is a best response to ρ_n. Formally, ρ_n is a Nash equilibrium if*

$$i \in \underset{j\in\mathcal{S}}{\operatorname{argmax}} F_j(\rho_n), for\ all\ i \in \mathcal{S}, \rho_i > 0,$$

where $\mathcal{S}$ is the discrete strategy set and $F_i : \mathcal{P}(\mathcal{S}) \to \mathbb{R}$ is the payoff to strategy i.

An equilibrium state should persist if undisturbed, since all strategies are equally fit, i.e., the payoff of all strategies will be the same. Nevertheless, in the realistic sense such as the epidemic evolution, the equilibrium is almost definitely disturbed, so that we are only interested in state which can return to the equilibrium when disturbed. This kind of equilibrium is said to be stable or satisfy the Nash stationarity (NS) [12] as follows.

Definition 2. *Evolutionary dynamics are said to satisfy the Nash stationarity if the Nash equilibrium of population game P coincides with the rest points of the evolutionary dynamics. Formally, the Nash Stationarity is*

$$d\rho_n = 0 \text{ if and only if } \rho_n \in NE(P),$$

where $d\rho_n$ is the gradient of equilibrium ρ_n.

With above preliminaries, we summarize the differences between MFED and RD as follows:

- **Population Flow**: RD only describes an unidirectional population flow while MFED allows a bidirectional population flow, which help us remove the unrealistic assumption that infected individuals can always get permanent immunity after recovery.
- **Graph Structure**: There are detailed graph structures in the MFED, providing abundant adjustable parameters for data fitting, while RD does not consider the graph structure.
- **Nash Stationarity**: MFED always satisfies NS but the RD fails to satisfy NS because it admits boundary points that are not the Nash equilibrium of the underlying game [12].

IV. Modeling the Transmission of COVID-19

A. Data Set and Evaluation Metrics

1) Data set: We collect the statistics of COVID-19 from the National Health Commission of People's Republic of China, the Chinese Center for Disease Control and Prevention , as well as the coronavirus research center in the Johns Hopkins University. As shown in Table I, from Jan. 20th to Feb. 11th, statistics cannot reflect the realistic transmission of COVID-19, mainly due to the unsophisticated detection method and insufficient serving capacity of hospitals at the early stage. On Feb. 12th, huge increment in the confirmed cases revealed the fact that patients infected by COVID-19 can be confirmed and reported precisely after the construction of hospitals and development of detection method. The number of infections reached the peak value on Feb. 18th and decreased to 0, for the first time, on Apr. 25th. Statistics remained unchanged between Apr. 25th and May. 8th. Therefore, we utilize the data between Feb. 12th and Apr. 25th to construct our model and test its accuracy.

TABLE I: Statistics of COVID-19 in Wuhan, China

Date	Confirmed	Infection	Death	Recovery
Jan. 20th	258	230	3	25
Feb. 10th	18,454	16,500	748	1,206
Feb. 11th	19,558	17,361	820	1,377
Feb. 12th	32,994	30,043	1,036	1,915
Feb. 18th	44,412	38,020	1,497	4,895
Apr. 25th	50,333	0	3,869	46,464
May. 8th	50,333	0	3,869	46,464

2) Evaluation metrics: The coefficient of determination (R^2) and the average relative bias are employed to evaluate the goodness of the fitting results. R^2 measures how successful the fit is in explaining the variation of the data, which is computed by

$$R^2 = 1 - \frac{\sum_{i=1}^{n} w_i (y_i - \hat{y}_i)^2}{\sum_{i=1}^{n} w_i (y_i - \bar{y})^2},$$

where y_i, $\hat{y}_i$, and $\bar{y}$ are the observed value, estimated value, and mean of observed value, respectively. The average relative bias is computed by

$$Bias = \frac{1}{n} \sum_{i=1}^{n} \frac{|y_i - \hat{y}_i|}{|y_i|}.$$

B. Transmission of COVID-19 in the SIDR Model

In the simulation, the statistics of COVID-19 on Feb. 12th are serving as the initial values for the SIDR model. The total population size is assumed to be $N = 50,333$, which is the final total confirmed cases on Apr. 20th, 2020. The effective reproduction number R_0 determines the potential of the pandemic, which is defined as the average number of secondary infections caused by a single infected individual. As suggested in [21], $R_0 = \eta N$ of COVID-19 should be between 2 and 2.5. Therefore, the infection rate η is set to 0.00004. According to the best-fit model parameters, the recovery rate and death rate are set to 0.021 and 0.03, respectively.

In Fig. 2a, we show the evolution of COVID-19 in the SIDR model. The transmission dynamics in (7) have been applied to update the population distribution on each state with $\omega_1 = 1$, $\omega_2 = 60$, and $\omega_3 = 1/8$. The peak number of the infected cases, the final number of recovered cases, and the final number of dead cases are $38,170$, $46,086$, and $3,609$, respectively. These critical values are close to the corresponding observed values shown in Table I.

C. Data Fitting

The trend of the number of infections could reveal the status of COVID-19 during its transmission process and help the government take actions to control the spreading of COVID-19 and reduce the economic losses. Thus, accurate prediction of it is of vital importance. The fitting results of the data of the infections, between Feb. 12th and Apr. 25th (74 days), have been shown in Fig. 2b. Dynamic adjustment of recover rate and death rate has been implemented to obtain better fitting results. The increment in recover rate and reduction in the

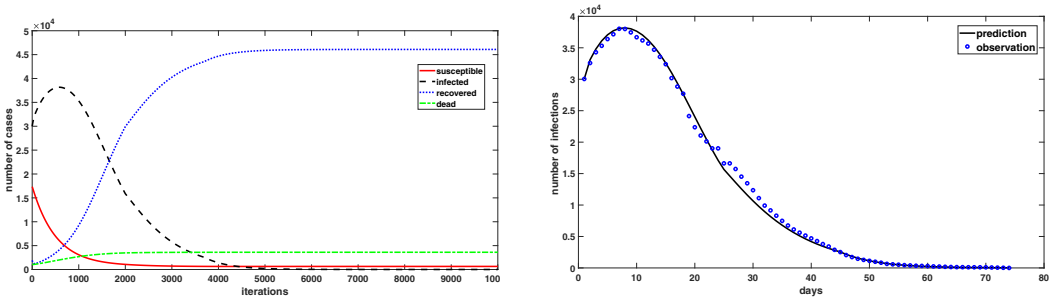

(a) Overall Transmission of COVID-19 (b) Fitting Results of the Infections

Fig. 2: Evolution of COVID-19 in the SIDR model

death rate are based on the fact that the treatment condition and the serving capacity of the hospitals have been gradually improved after the effort of the government. The values of two evaluation metrics are

$$R^2 = 0.9969, \quad \text{and} \quad Bias = 0.0953,$$

which proves that the SIDR model, with the MFED as the transmission dynamics, achieves good fitting results.

D. Effect of One-time Social Distancing

Social distancing (SD) measures are assumed to be taken at the beginning of the COVID-19 outbreak. The duration of SD, denoted in the blue region in Fig. 3, varies from two months to indefinite period. The reduction on the infection rate varies from 0 to 80% representing the different strengths of SD.

As shown in Fig. 3, different strengths of SD can lead to different level of reduction on the peak number of infections, which is significant to restrain the spreading of COVID-19. After high strength of SD, which can result in 80% reduction on the infection rate shown in the green curve, a surge of infections will appear if the population return to the normal social distance suddenly. The critical reason behind this phenomenon is that only very few people in the population can obtain the immunity to COVID-19 under high strength of SD. Therefore, step-by-step reopening of businesses and schools is highly recommended to avoid a second outbreak.

E. Seasonality of COVID-19 through the post-pandemic period

Seasonality analyses of COVID-19 have been shown in Fig. 4. We use d_0 to denote the length of time when one recovered individual can maintain the immunity and L_0 to denote the proportion of population who will loss their immunity. v_0 refers to the variation of the basic infection rate in winter and in summer.

In Fig. 4a, periodic outbreak of COVID-19 has been depicted for $d_0 = 6$ months and $d_0 = 12$ months. The immunity loss is $L_0 = 0.8$, i,e., 80% of the recovered population will lose their immunity after the duration d_0. There is no seasonal variation ($v_0 = 1$). The peak number of infections will gradually decrease through the outbreaks. A long duration $d_0 = 12$ months of COVID-19 immunity can yield annual outbreak of COVID-19. In Fig. 4b, we show the impact of the proportion of immunity loss on the seasonality of COVID-19. The immunity duration is set as $d_0 = 6$ months and there is no seasonal variation ($v_0 = 1$). The immunity loss L_0 varies from 0.4 to 0.8. Higher immunity loss will yield more severe outbreak of COVID-19 every half year. But no matter how many people will lose their immunity every half year, the peak number of infections will gradually decrease across the time. In Fig. 4c, the effect of seasonal variation has been shown. The immunity loss is $L_0 = 0.8$ and the duration is $d_0 = 6$ months. The infection rate is η during the winter time and $v_0\eta$ during the summer time, where v_0 could be 0.2 or 0.8. The winter of 2019 is regarded as the starting point. Higher seasonal variation would significantly reduce the peak number of infections in the summer time but yield a more severe outbreak of COVID-19 in the following winter. The overall trend of the peak number of infections is still decreasing.

V. Conclusion

Mean field evolutionary dynamics, inspired by optimal transport and mean field games on graphs, has been proposed to model the evolution of COVID-19. It has been compared with the exclusively-utilized replicator dynamics theoretically. Allowing bidirectional population flow, satisfying the Nash stationarity, and containing detailed graph structures, are its superior characteristics. Applied to the SIDR model, the mean field evolutionary dynamics fit very well into the real statistics, with coefficient of determination $R^2 = 0.9969$ and $Bias = 0.0953$. One-time social distancing can reduce the peak number of infections significantly. However, a second outbreak of COVID-19 will arise after a high strength of social distancing. Finally, people's limited length of immunity will yield a periodic outbreak of COVID-19 and higher seasonal variation of infection rates will reduce the infections in summer but lead to a more severe outbreak in the following winter.

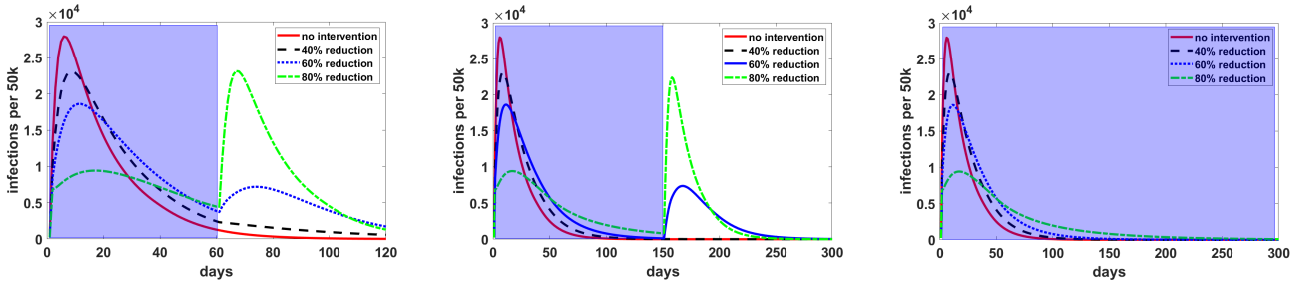

(a) Two months (b) Five months (c) Indefinite

Fig. 3: One-time social distancing in the absence of seasonality

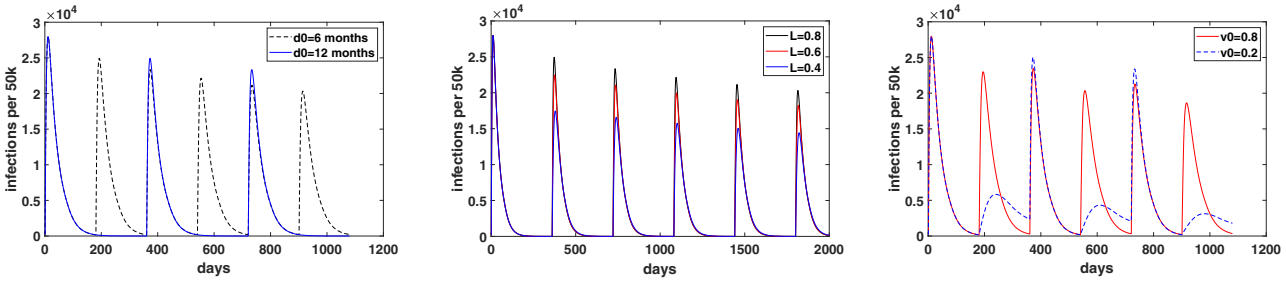

(a) Effect of the immunity duration (b) Effect of the proportion of immunity loss (c) Effect of seasonal variation

Fig. 4: Seasonality Analysis of COVID-19

REFERENCES

[1] "Financial impact of the 2019–20 coronavirus pandemic," Mar. 2020. [Online]. Available: https://en.wikipedia.org/wiki/Financial_impact_of_the_2019%E2%80%9320_coronavirus_pandemic

[2] "Coronavirus live update," Apr. 2020. [Online]. Available: https://news.qq.com/zt2020/page/feiyan.htm?kw=ad_sy#/area

[3] "Coronavirus resource center," Apr. 2020. [Online]. Available: https://coronavirus.jhu.edu/map.html

[4] W. O. Kermack and A. G. McKendrick, "A contribution to the mathematical theory of epidemics," *Proceedings of the Royal Society of London. Series A, Containing Papers of a Mathematical and Physical Character*, vol. 115, no. 772, pp. 700–721, 1927.

[5] E. Gubar and Q. Zhu, "Optimal control of influenza epidemic model with virus mutations," in *Proceedings of the European Control Conference (ECC)*, Zurich, Switzerland, Jul. 2013, pp. 3125–3130.

[6] M. De la Sen, S. Alonso-Quesada, and A. Ibeas, "On the stability of a delayed SEIR epidemic model with feedback vaccination controls," in *Proceedings of the International Conference on BioSignal Analysis, Processing and Systems (ICBAPS)*, Kuala Lumpur, Malaysia, May 2015, pp. 61–66.

[7] I. Nino, M. Fernandez, M. De la Sen, S. Alonso-Quesada, R. Nistal, and A. Ibeas, "About two compared SEIADR and SEIR discrete epidemic models," in *Proceedings of the 17th International Conference on ICT and Knowledge Engineering (ICT KE)*, Bangkok, Thailand, Nov. 2019.

[8] P. D. Taylor and L. B. Jonker, "Evolutionary stable strategies and game dynamics," *Mathematical Biosciences*, vol. 40, no. 1-2, pp. 145–156, 1978.

[9] I. Gilboa and A. Matsui, "Social stability and equilibrium," *Econometrica*, vol. 59, no. 3, pp. 859–67, 1991.

[10] G. W. Brown and V. Neumann, *Solutions of Games by Differential Equations In: H. W. Kuhn and A. W. Tucker, Eds.* Princeton University Press, 1950.

[11] M. J. Smith, "The stability of a dynamic model of traffic assignment—an application of a method of lyapunov," *Transportation Science*, vol. 18, no. 3, pp. 245–252, 1984.

[12] S. William, "Pairwise comparison dynamics and evolutionary foundations for nash equilibrium," *Games*, vol. 15, pp. 3–17, Mar. 2009.

[13] R. Eletreby, Y. Zhuang, K. M. Carley, O. Yağan, and H. V. Poor, "The effects of evolutionary adaptations on spreading processes in complex networks," *Proceedings of the National Academy of Sciences*, vol. 117, no. 11, pp. 5664–5670, 2020.

[14] S. Chow, W. Li, and H. Zhou, "Entropy dissipation of Fokker-Planck equations on finite graphs," *Discrete & Continuous Dynamical Systems*, vol. 38, no. 10, pp. 4929–4950, Jul. 2018.

[15] H. Gao, W. Li, R. A. Banez, Z. Han, and H. V. Poor, "Mean field evolutionary dynamics in ultra dense mobile edge computing systems," in *Proceedings of the 2019 IEEE Global Communications Conference (GLOBECOM)*, Hawaii,USA, Dec. 2019, pp. 1–6.

[16] W. Li, "Transport information geometry i: Riemannian calculus on probability simplex," *arXiv:1803.06360*, Mar. 2018.

[17] S.-N. Chow, W. Li, J. Lu, and H. Zhou, "Equilibrium selection via optimal transport," *SIAM Journal on Applied Mathematics*, vol. 80, pp. 142–159, Jan. 2020.

[18] D. Shi, H. Gao, L. Wang, M. Pan, Z. Han, and H. V. Poor, "Mean field game guided deep reinforcement learning for task placement in cooperative multi-access edge computing," *IEEE Internet of Things Journal*, to appear.

[19] Q. Cheng, L. Li, K. Xue, H. Ren, X. Li, W. Chen, and Z. Han, "Beam-steering optimization in multi-uavs mmwave networks: A mean field game approach," in *Proceedings of the 2019 11th International Conference on Wireless Communications and Signal Processing (WCSP)*, 2019, pp. 1–5.

[20] C. Yang, Y. Zhang, J. Li, and Z. Han, "Power control mean field game with dominator in ultra-dense small cell networks," in *Proceedings of the 2017 IEEE Global Communications Conference*, 2017, pp. 1–6.

[21] S. M. Kissler, C. Tedijanto, E. Goldstein, Y. H. Grad, and M. Lipsitch, "Projecting the transmission dynamics of SARS-CoV-2 through the postpandemic period," *Science*, vol. 368, no. 6493, pp. 860–868, 2020.